

Pathway-dependent fate of permafrost region carbon: Supplementary Information

Thomas Kleinen and Victor Brovkin

13th July 2018

Max Planck Institute for Meteorology, Bundesstr. 53, 21107 Hamburg, Germany,
thomas.kleinen@mpimet.mpg.de

1 Supplementary Figures for methods section

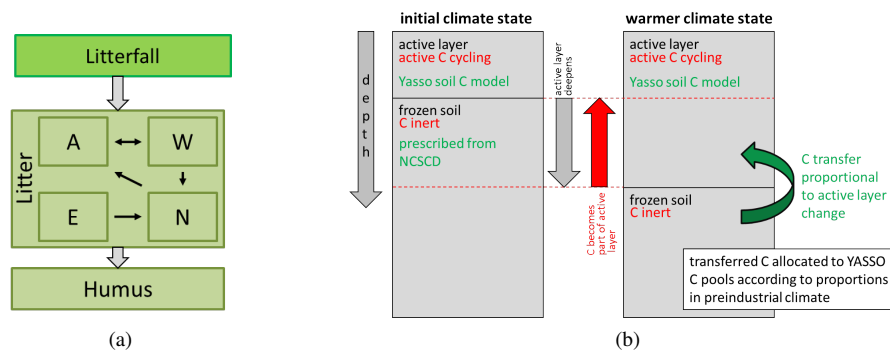


Figure S1: Simplified representation of the carbon pool structure in YASSO (a) and schematic of the carbon transfer as active layer thickness changes (b).

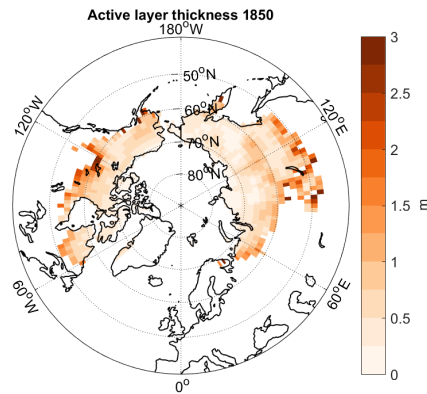


Figure S2: JSBACH active layer thickness in preindustrial (1850) climate.

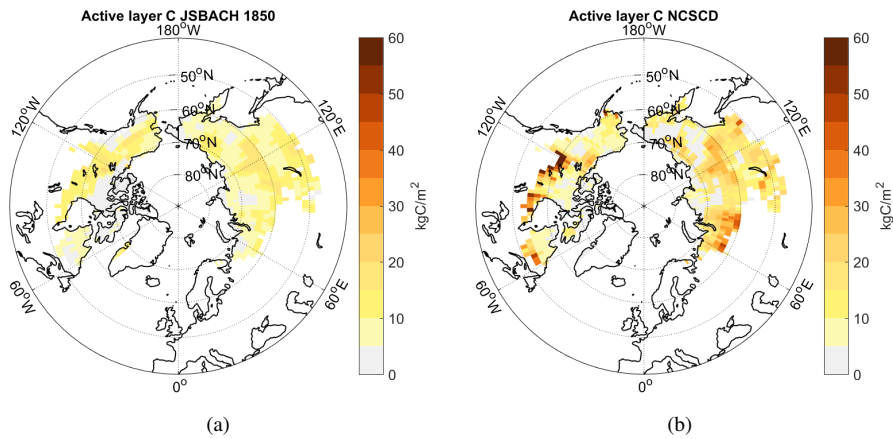


Figure S3: Carbon in the active layer in (a) JSBACH preindustrial (1850) state and (b) NCSCD. Active layer thickness diagnosed from JSBACH for 1850, as shown in Fig. S2.

2 Results

2.1 Permafrost region temperature

The annual mean temperature of the permafrost region (Fig. S4) is about -9.3°C in preindustrial climate. It increases to -7.5°C in 2005 and continues to increase until 2300 in RCPs 4.5 and 8.5, reaching final values of -2.8°C and 9.5°C , respectively. In RCP 2.6, however, permafrost region temperature peaks at -4.7°C in 2044 and declines thereafter, reaching -7.1°C in 2300.

2.2 Permafrost carbon thaw

Permafrost thaw implies an increase of the depth of the active layer (AL), the soil layer thawing during the summer season. As the thaw deepens, the carbon contained in soil

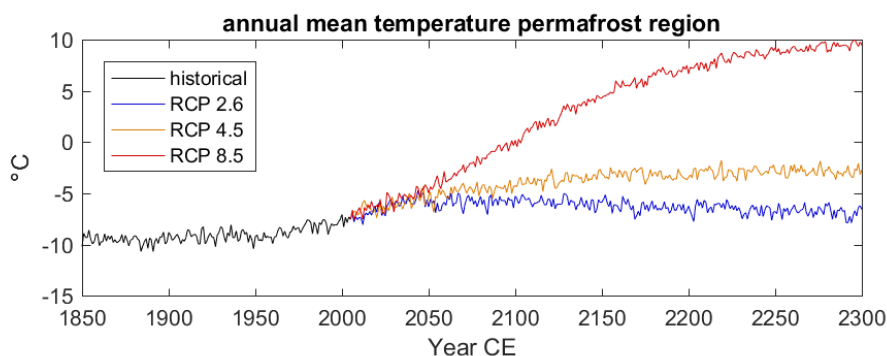


Figure S4: Annual mean surface air temperature, average for the permafrost region.

layers that were perennially frozen previously becomes available to active carbon cycling. We model this process by transferring carbon from the prescribed frozen C pools to the active layer C pools, as described in the methods section. In our experiments, climate warms during the 21st and 22nd centuries, with permafrost region annual mean temperatures increasing to above freezing in RCP 8.5 (Fig. S4), while area mean temperatures remain below freezing in RCPs 2.6 and 4.5.

During the historical period the frozen carbon stock changes slowly, declining from 691 PgC in 1850 to 630 PgC in 2005 (Fig. 1a, main text). Following RCP 2.6 into the future, the frozen carbon stock declines from the 2005 value to about 495 PgC in 2075 and changes very little afterwards, with a final value of 485 PgC in 2300. Conceivably the frozen C stock might increase again slightly, due to re-freezing of formerly thawed soil layers. This effect, however, is not considered in the model, as we see very small decreases in active layer thickness. Following scenario RCP 4.5, the decline is substantially stronger and continues into the 22nd and 23rd century, with a final frozen C stock of 325 PgC in 2300. In scenario RCP 8.5 the entire frozen C stock is mobilised during the experiment, as annual mean temperatures in the permafrost region rise above the freezing point (Fig. S4). 65% of the carbon is thawed by 2100, and most of the remainder thaws during the 22nd century, with very little carbon left in frozen state by 2200 and no carbon remaining frozen by the end of the experiment in 2300.

Carbon in the active layer of the permafrost region increases considerably in the experiments, even if the carbon in permafrost is not considered. The active layer C pools in the non-permafrost experiments, shown as dashed lines in Fig. 1b (main text), increase from 162 PgC at preindustrial to 178 PgC in 2005, and then increase further in the scenario experiments. For 2200 they reach values of 226 PgC in RCP 2.6, 255 PgC for RCP 4.5, and 272 PgC for RCP 8.5. During the last century of our experiment they increase further to 287 PgC for RCPs 4.5 and 8.5, but stay roughly constant for RCP 2.6. If permafrost carbon is considered, shown as solid lines in Fig. 1b (main text), the carbon stored in the formerly frozen soil layers is transferred to the actively cycling C pools, increasing the active layer carbon pools significantly. For the historical period active layer carbon increases to 230 PgC in 2005, 52 PgC more than if permafrost C is not considered. Following RCP 2.6, active layer C increases to 345 PgC in 2075, but declines slowly thereafter, with a final value of 329 PgC reached in 2300. In RCP 4.5 active layer C increases continuously until 2300, when a final amount of 469 PgC

is reached. Following RCP 8.5, a maximum of 665 PgC is reached in 2164, slowly decreasing afterwards, with a final value of 590 PgC in 2300. Of the carbon mobilised by permafrost thaw, about twice as much carbon is allocated to the slowly cycling humus C pool as to the quickly cycling litter C pools (Fig. S5), while the soil carbon increase is mainly allocated to the litter C pools if permafrost C is not considered. These changes, as well as changes to the carbon fluxes, are summarised in Table 1 (main text).

2.3 Allocation of thawed permafrost C

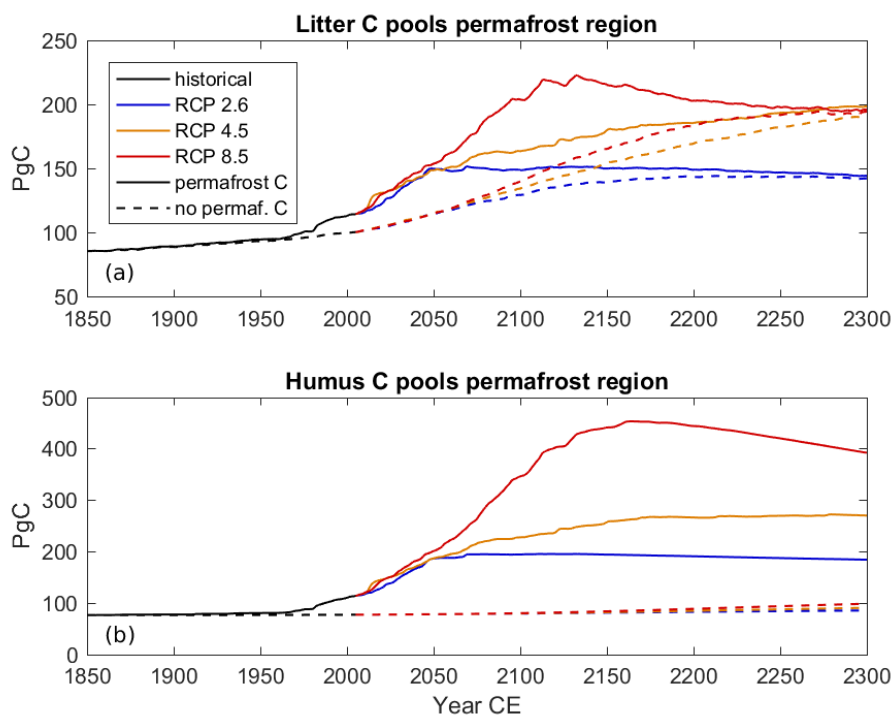


Figure S5: Active layer carbon pools in 1850-2300 following scenarios RCP 2.6, RCP 4.5, and RCP 8.5. (a) litter C pools, (b) humus C pool. Solid lines show experiments with frozen permafrost C considered, dashed lines experiments without permafrost C.

The YASSO model distinguishes between soil carbon in litter C pools and in a humus C pool. The litter C pools are based on the solubility of litter in different media, the litter C decompose on time scales of months to years, while the humus C pool decomposes on a timescale of centuries. Soil carbon added through litterfall from the vegetation is initially added to the litter C pools, while the humus pool builds up from products of litter decomposition. In an equilibrium climate an equilibrium distribution of soil carbon is reached after several millennia. If climate in the model is perturbed, changes in vegetation will first change the content of the litter C pools, while the adjustment of the humus C pools will take several centuries.

In the initial climate state in 1850, the permafrost region contains 86 PgC in the

litter C pools and 77 PgC in the humus C pools. Without permafrost C this increases to 101 PgC for litter C at the end of the historical period in 2005, while humus C does not change. Litter C, shown as a dashed line in Fig. S5a, continuously increases in RCP 2.6 up until 2212, where a maximum of 144 PgC is reached, subsequently decreasing to 142 PgC in 2300. In RCP 4.5 this increase is larger, reaching a final value of 191 PgC in 2300, and in RCP 8.5 the final value is 194 PgC. Humus C, shown in Fig. S5b, changes very little in the non-permafrost C experiments, showing an increase to 98 PgC for RCP 8.5 and smaller increases for the other two scenarios.

Carbon mobilised from thawing permafrost differs from carbon added through litterfall in that it is previously formed soil carbon that is frozen in place, implying that it contains not just litter C, but also humus C. Since few constraints for pool allocations are available, we assume that active layer carbon in the preindustrial state is representative of the soil carbon at the time of permafrost C freeze. Therefore carbon thawed from permafrost is assumed to have the same ratio of single pool carbon to total carbon and is added to the YASSO soil C pools accordingly. As a result, increases in soil carbon from permafrost thaw affect both the litter and the humus C pools. At the end of the historical period in 2005, litter C pools therefore increase to 115 PgC and humus pools increase to 114 PgC. Under RCP 2.6, shown as a solid line in Fig. S5a, litter C increases to a maximum of 151 PgC, reached in 2131, subsequently declining to 144 PgC in 2300, while humus C, shown in Fig. S5b, increases to a maximum of 195 PgC, reached in 2117, declining thereafter to 184 PgC in 2300. Under RCP 8.5 the development is qualitatively similar, though the numbers are larger: The maximum in litter C is 221 PgC, reached in 2134, declining to 196 PgC in 2300, and the maximum in humus C is 452 PgC, reached in 2168, declining to 394 PgC in 2300. Under RCP 4.5 the maximum is reached at the end of the experiment in 2300, with a total litter C pool of 198 PgC and a total humus C pool of 270 PgC.

Of the thawed permafrost carbon a substantial fraction therefore goes into the slowly decomposing humus carbon pools, leading to a long-term carbon release from the humus pools, but substantially reducing the short-term release. The total soil carbon in the active layer (Fig. 1b, main text), reflects the changes in the constituents: when considering permafrost C, the change in active layer C is caused by changes in litter and humus pools, which both increase strongly due to the addition of thawed permafrost carbon. Without permafrost carbon the change in active layer C is mainly determined by the changes in litter C caused by the increased productivity under global warming.

2.4 Carbon fluxes

While the increases in active layer carbon will affect carbon fluxes to the atmosphere through changes in heterotrophic respiration (R_h), or soil carbon decomposition, this is only part of the carbon balance of the permafrost region. The climatically relevant measure is rather the net carbon flux into the permafrost region, which is comprised of net primary productivity (NPP), heterotrophic respiration R_h , and further carbon fluxes, such as land use change, fire emissions, and herbivory. The latter fluxes are small in comparison to NPP and R_h , and we combine them with R_h for the following discussion. The net C balance of the permafrost region therefore is $NPP - R_h$. NPP in the permafrost region is affected by the atmospheric CO_2 concentration and temperature, mainly through growing season length. R_h , on the other hand, is mainly dependent on temperature and the amount of C available for decomposition.

Over the historical period 1850-2005, NPP in the permafrost region (Table 1 (main

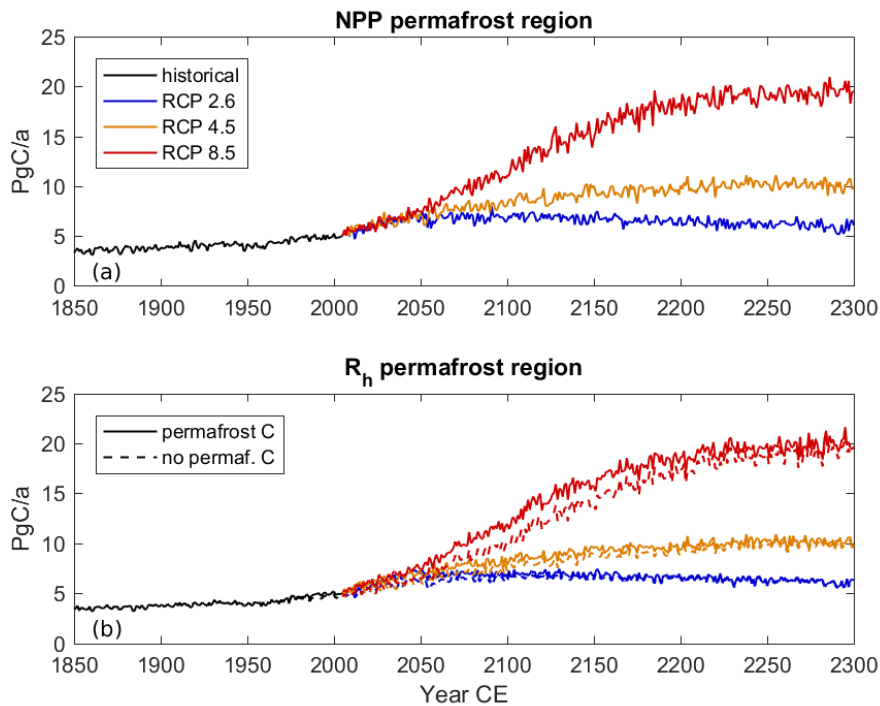


Figure S6: Net primary productivity (NPP, a) and heterotrophic respiration (R_h , b) in the permafrost region for historical climate and RCP scenarios. NPP is identical with and without the consideration of permafrost C. For R_h , solid lines show the cases with permafrost C, dashed lines are without permafrost C.

text) and Fig. S6a) increases from 3.5 PgC/a to 5.1 PgC/a in our experiments, due to climate warming and CO_2 -fertilisation. R_h (Fig. S6b) increases from 3.5 PgC/a to 5.1 PgC/a (4.8 PgC/a), if permafrost C is considered (ignored), leading to a constant net C flux with permafrost C or an increase to 0.3 PgC/a without permafrost C.

In the subsequent scenario experiments, NPP under RCP 2.6 increases to a maximum of 7.0 PgC/a in 2045, with a subsequent decline to 6.0 PgC/a in 2300. Similarly, R_h increases to a maximum of 7.1 PgC/a (6.7 PgC/a) in 2047 (2152) with (without) permafrost C. R_h decreases subsequently, with very small differences between the cases with and without permafrost C after 2100 and a final value of 6 PgC/a in 2300. As a result of the changes in the flux components, the net C flux decreases (increases) with (without) permafrost C to a minimum (maximum) of -0.3 PgC/a (0.7 PgC/a), increasing (decreasing) again to -0.1 PgC/a (0 PgC/a) in 2300.

The behaviour is qualitatively different in RCPs 4.5 and 8.5, where CO_2 does not decrease, but is stabilised. Under these scenarios NPP continues to increase to the end of the experiments, reaching final values of 10.1 PgC/a and 19.5 PgC/a, respectively, under RCP 4.5 and RCP 8.5. For heterotrophic respiration R_h RCPs 4.5 and 8.5 are qualitatively different from RCP 2.6 as well, showing increasing values to the end of the experiments. In RCP 4.5, R_h reaches a maximum of 10.2 PgC/a (9.8 PgC/a) in the (non-)permafrost case. The difference between the two cases is at most 0.8 PgC/a, reached in 2075. As a consequence, the net C flux with permafrost C varies between

0.2 PgC/a and -0.2 PgC/a, with a final value of -0.1 PgC/a in 2300, while it increases without permafrost C to 0.9 PgC in 2067, subsequently decreasing to 0.3 PgC/a in 2300. Finally, in RCP 8.5 the maximum difference in R_h between the cases with and without permafrost of 2.2 PgC/a is reached in 2114 and declines thereafter. Here, R_h increases to a final value of 19.9 PgC/a (19.2 PgC/a) with (without) permafrost C. As a consequence, the net C flux with permafrost C decreases to -0.9 PgC/a in 2135 and subsequently increases again to -0.4 PgC/a in 2300; without permafrost C it increases to a maximum of 1.6 PgC/a in 2127 and subsequently declines to 0.3 PgC/a in 2300.

Without considering permafrost C the climatically relevant net carbon flux $NPP - R_h$ therefore is generally positive, indicating a net uptake of carbon by the land surface, with the exception of RCP 2.6 after 2200. When considering permafrost C, however, the net C fluxes are strongly reduced and generally are negative. Cumulatively, this adds up to significant changes in climate forcing, shown in Fig. 2 (main text). Without permafrost C, the cumulative net flux for RCP 2.6 reaches a maximum of 85 PgC in 2195, decreasing thereafter to 79 PgC in 2300, while the cumulative net flux increases continuously for RCPs 4.5 and 8.5, where maxima of 185.2 and 284.6 PgC, respectively, are reached in 2300. If permafrost C is considered, however, the cumulative net fluxes decrease significantly in all experiments. For RCP 2.6 the cumulative net flux in 2300 is -23.6 PgC, reduced by 102.8 PgC due to respired permafrost carbon in comparison to the non-permafrost case. In RCP 4.5, the cumulative net flux to 2300 is 9.6 PgC with permafrost C, i.e. an uptake reduction by 175.6 PgC. Finally in RCP 8.5 the cumulative net flux up until 2300 is -104 PgC when considering permafrost C, implying a reduction in uptake by 388.6 PgC.

In all scenarios the net flux therefore is reduced significantly, with the permafrost region turning from a sink of carbon to a source in RCPs 2.6 and 8.5, while it remains a (very small) sink in RCP 4.5. The positive cumulative net flux in RCP 4.5 is a rather special case and due to the exact nature of the scenario: The overall warming in RCP 4.5 is small enough for part of the permafrost C to remain frozen, leading to less thawed C being available for decomposition than in RCP 8.5. At the same time atmospheric CO_2 is stabilised in RCP 4.5, leading to continuously increasing NPP, while CO_2 declines in RCP 2.6, leading to a decrease in NPP after 2045.

2.5 Spatial pattern of net C fluxes

The spatial pattern of cumulative net C fluxes upon permafrost thaw is closely related to the spatial pattern of carbon stocks in the NCSCD. These stocks are largest in areas of organic soils (Fig. S7a), and the spatial pattern directly translates into the magnitude of the cumulative net C fluxes (Fig. S7b). However, the representation of soils in land surface models is limited, and the special conditions leading to the preservation of organic material in organic soils cannot be modelled in a satisfactory way. Especially the question whether water-logged conditions, which led to the preservation of the organic material, remain under changed climatic conditions cannot be addressed properly in the current generation of land surface models, as these lack the representation of processes vital to organic soil formation and are designed for a spatial scale too coarse for a good representation.

2.6 Effects of CO_2 and climate

In order to separate the effects of CO_2 and climate changes on the permafrost region C balance, we performed additional experiments for the historical period, as well as

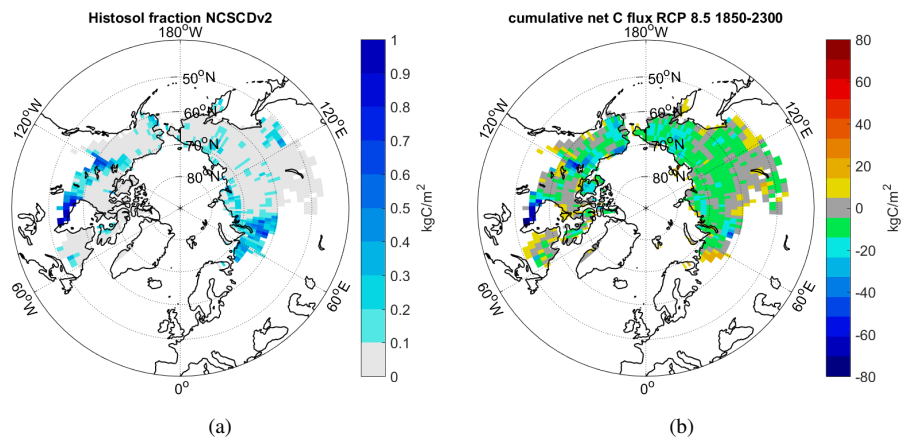


Figure S7: Grid cell fraction of organic soils in NCSCD (a) and spatial distribution of cumulative net C flux in RCP 8.5 with permafrost C (b).

RCPs 2.6 and 4.5. In these experiments, we forced the model with CO_2 forcing according to the scenario, but preindustrial climate (named “ CO_2 ”), or with preindustrial CO_2 and climate forcing according to the scenario (named “Climate”). CO_2 and climate have distinct effects in the permafrost region carbon balance. In the Farquhar et al. [1980] photosynthesis model used in JSBACH, as well as in numerous other vegetation models, an increase in atmospheric CO_2 (to be precise: an increase in the CO_2 concentration at the leaf surface) leads to an increase in carbon assimilation per absorbed radiation. Climate change, with temperature increase the most important factor in the present discussion, leads to three changes in permafrost region C cycling: 1) permafrost thaw leads to the mobilisation of C stored in frozen soil layers, 2) assuming constant soil C, a temperature increase leads to an increase in heterotrophic respiration as the respiration is temperature-dependent, and 3) a temperature increase prolongs the growing season as snow melts earlier in the spring and falls later in the autumn. This latter effect of climate change also has a synergy with CO_2 increase: As the growing season is lengthened, the effect of higher CO_2 concentrations on photosynthesis becomes enhanced as more time is available for assimilating carbon.

In our factor separation experiments we see that NPP reacts to both changes in CO_2 and to changes in climate (Fig. S8a and Table S1). At the relatively low warming levels of the historical period and RCP 2.6, NPP is very similar in the CO_2 and climate only forcing experiments, though lower than in the full forcing experiment. NPP peaks in the late 21st century and declines thereafter in both forcing factor experiments. For RCP 4.5, the NPP increase after 2150 becomes larger in the climate only experiment than in the CO_2 only experiment. Please note that there is a significant synergy between the CO_2 and climate forcings: For RCP 4.5 the NPP increase from 1850 to 2300 in the full forcing experiment is 6.6 PgC/a, while the increase in the CO_2 only experiment is 2.3 PgC/a and the increase in the climate only experiment is 2.9 PgC/a. The difference between the sum of the single forcing experiments and the full forcing experiments – 1.4 PgC/a – is due to the synergy between the single forcings. The mechanism for the synergy is as follows: Climate change on its own leads to a longer growing season, and the CO_2 increase on its own leads to an increase in carbon fixation per photon absorbed. Thus the combined forcing leads to an enhanced carbon fixation effective

Scenario	ΔNPP [PgC/a]	ΔR_h [PgC/a]	$\Delta\text{net C}$ [PgC/a]	$\Delta\text{cum. net C}$ [PgC]	$\Delta\text{frozen C}$ [PgC]	$\Delta\text{AL C}$ [PgC]
2005						
hist CO ₂	0.9	0.6	0.2	11.3	-4	16
hist Clim.	0.8	1.0	-0.3	-6.3	-63	59
hist Syn.	0.0	0.0	0.1	2.8	5	-8
2050						
2.6 CO ₂	1.4	1.1	0.2	23.8	-4	26
2.6 Clim.	1.5	2.0	-0.6	-25.3	-180	152
2.6 Syn.	0.4	0.2	0.2	9.9	7	-7
2100						
2.6 CO ₂	1.5	1.2	0.1	31.8	-4	34
2.6 Clim.	1.5	1.7	-0.2	-43.8	-202	151
2.6 Syn.	0.4	0.3	0.1	17.7	8	-4
4.5 CO ₂	2.1	1.5	0.3	40.0	-4	39
4.5 Clim.	2.0	2.2	-0.4	-56.1	-256	191
4.5 Syn.	0.8	0.6	0.2	23.5	7	-2
2300						
2.6 CO ₂	1.1	1.0	0.0	25.1	-4	36
2.6 Clim.	1.3	1.2	-0.1	-76.4	-210	130
2.6 Syn.	0.1	0.2	0.0	27.8	9	0
4.5 CO ₂	2.3	1.9	0.1	60.6	-4	61
4.5 Clim.	2.9	3.0	-0.2	-113.8	-366	226
4.5 Syn.	1.4	1.3	0.1	62.9	5	19

Table S1: Contributions of CO₂, Climate, and Synergy to changes in C fluxes and pools in comparison to preindustrial for RCPs 2.6 and 4.5. Values are given for 2005, 2100, and 2300, with 2050 also given for RCP 2.6.

over a longer growing season, increasing C assimilation by a larger amount than the single factors would suggest. This also leads to a stronger reduction in NPP in the RCP 2.6 full forcing experiment after the CO₂ peak in 2050, as lower atmospheric CO₂ concentrations combine with a shortening growing season as climate cools slightly.

For the active layer C pools, we see a slow increase in the litter C pools (Fig. S9a) throughout the historical and scenario periods in the experiments forced by CO₂ only, as the increase in NPP through CO₂-fertilisation leads to increases in biomass and thereafter to increases in litterfall. For the two scenario experiments forced by CO₂ only, the trajectories diverge after 2050, when CO₂ in the RCP 2.6 scenario starts decreasing again, with final values in 2300 of 115 PgC and 137 PgC for RCP 2.6 and RCP 4.5, respectively (Table S1). Driven by climate only, the increases in litter C initially are larger than in the CO₂-only case, as thawing permafrost C gets added to the litter C pools. For RCP 2.6 litter C peaks in 2050 at 129 PgC, decreasing to 112 PgC in 2300 thereafter, while litter C stabilises around 128 PgC after 2080 in the RCP 4.5 scenario (Table S1). Once again the synergy between CO₂ and climate change is substantial, leading to larger litter C pools under full forcing than the sum of the single forcing factors would suggest. For humus C the model shows a slightly increasing trend in the CO₂ only experiments, due to the slow incorporation of litter C into the humus pools, but changes in the experiments driven by climate are more pronounced

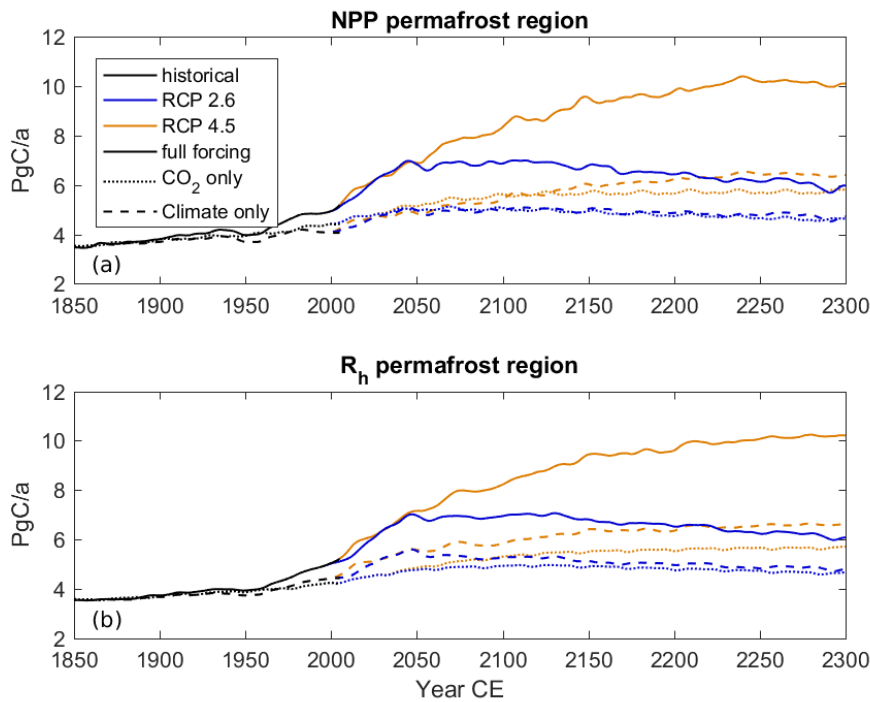


Figure S8: Net primary productivity (NPP, a) and heterotrophic respiration (R_h , b) in the permafrost region for historical climate and RCP scenarios 2.6 and 4.5, with full forcing, and CO₂ and climate forcings separated. Solid lines show experiments with full (CO₂ and climate) forcing, dotted lines CO₂ forcing only, dashed lines climate forcing only.

due to the incorporation of thawed permafrost C into the humus C pools.

Heterotrophic respiration, finally, shows a stronger reaction to climate change than to CO₂ change (Fig. S8b). In the case of the CO₂-only forcing, the increases in NPP due to CO₂-fertilisation are translated into increases in active layer carbon, as discussed above, which in turn leads to an increase in R_h . For RCP 2.6 the result is an increase in R_h until about 2100, after which R_h stays more or less constant at 4.9 PgC/a, while R_h keeps increasing in RCP 4.5 until a final value of 5.7 PgC/a is reached in 2300. Climate change, on the other hand leads to an increase in R_h due to two factors: Active layer C increases due growing season lengthening and permafrost thaw, as discussed above, and R_h is accelerated through the temperature dependence of respiration itself. R_h with climate-only forcing thus peaks in RCP 2.6 at 5.7 PgC/a in 2050, decreasing thereafter to 4.8 PgC in 2300, while it keeps increasing to a final value of 6.6 PgC/a in RCP 4.5. For R_h , too, significant synergy between CO₂ and climate change can be observed, as the increase in R_h between 2850 and 2300 under RCP 4.5 is 2.2 PgC/a with CO₂-only forcing and 3.1 PgC/a with climate-only forcing, but 6.7 PgC/a with the combined forcings.

As a result, the cumulative net C flux into the permafrost region (Fig. S10) is generally positive under CO₂ forcing, as the increase in NPP from CO₂ fertilisation is larger than the increase in R_h , leading to a positive net C flux. Under climate-only forcing,

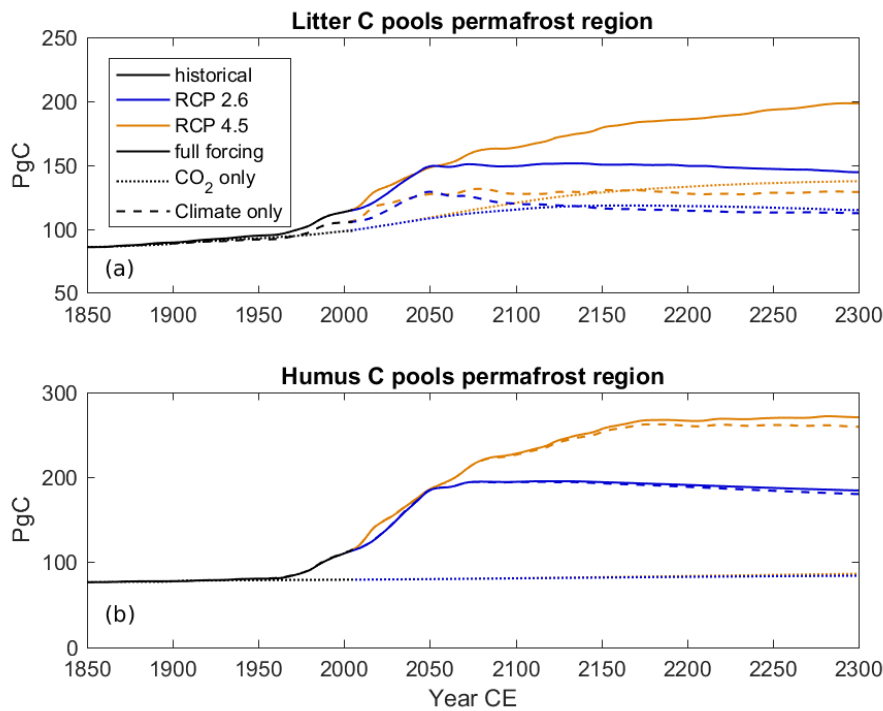


Figure S9: Active layer carbon pools in 1850-2300 following scenarios RCP 2.6 and RCP 4.5 with full forcing, and CO₂ and climate forcings separated. (a) litter C pools, (b) humus C pool. Solid lines show experiments with full (CO₂ and climate) forcing, dotted lines CO₂ forcing only, dashed lines climate forcing only.

on the other hand, the cumulative net C flux is generally negative, as the thawing of permafrost C and other increases in respiration outweigh the increase in NPP. Differences between the two scenarios are apparent in the net C flux, though: under RCP 2.6 the cumulative net C flux with CO₂-only forcing peaks in 2140 at 33 PgC, thereafter declining to 25 PgC in 2300, indicating a carbon release after 2140 as atmospheric CO₂ concentrations decline. Under RCP 4.5 no similar decline is apparent. In addition, the larger synergy between CO₂ and climate under RCP 4.5 leads to a stronger increase of the net C flux in comparison to the climate-only forcing experiment, leading to a small positive net C flux over the full forcing experiment.

References

- G. D. Farquhar, S. von Caemmerer, and J. A. Berry. A biochemical model of photosynthetic CO₂ assimilation in leaves of C3 species. *Planta*, 149(1):78–90, 1980. doi: 10.1007/BF00386231.

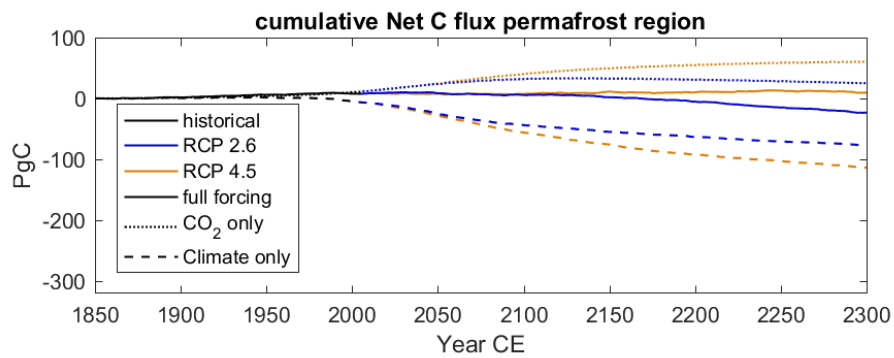


Figure S10: Cumulative net carbon flux into the permafrost region for historical and RCP scenarios 2.6 and 4.5, with full forcing, and CO₂ and climate forcings separated. Solid lines show experiments with full (CO₂ and climate) forcing, dotted lines CO₂ forcing only, dashed lines climate forcing only.